Progress in Chemical and Biochemical Research

Journal homepage: www.pcbiochemres.com

Original Research Article

Preparation, Electrochemical Characterization and Vapour Sensing Application of Nanoporous Activated Carbon derived from Lapsi

Armila Rajbhandari (Nyachhyon)*, Sandhya Acharya

Central Department of Chemistry, Tribhuvan University, Kirtipur, Kathmandu, Nepal

ARTICLE INFO

Article history

Submitted: 2020-07-15
Revised: 2020-08-16
Accepted: 2020-08-22
Available online: 2020-09-10
Manuscript ID: PCBR-2007-1110
DOI: 10.22034/pcbr.2020.113921

KEYWORDS

Activated carbon, Phosphoric acid activation, Electrochemical characterization, Vapour Sensing Application

ABSTRACT

Activated carbon (AC) has been successfully prepared from agricultural waste lapsi seed stone. The phosphoric acid activation was done by varying the ratio of H_3PO_4 and lapsi seed powder (LSP) from (0.9:1) to (1.5:1) which was followed by carbonization at 400°C in a tubular furnace under nitrogen atmosphere for 3 hrs. Besides this, precursor was preheated to 200°C for 2-6 hrs. Thus prepared material was characterized by BET N_2 adsorption- desorption process and showed high >1500 m^2/g surface area with high pore volume. The electrochemical characterization was carried out using three electrode system where carbon electrode was used as working electrode, platinum as counter electrode and Ag/AgCl electrode as a reference electrode. CV has been found operating in acidic electrolyte solution of (1 M) H_2SO_4. The results revealed a very promising capacitance value of 202 F/g at current density of 1 A/g. Charge–discharge measurement showed a good indication of stable cyclic performance up to 1000 cycles at current density of 5 A/g. Such electrochemical properties exhibited the high prospect for development of energy storage materials. As prepared activated carbon also showed excellent sensing ability towards vaporized solvent gases like methanol, acetone, benzene, hexane, pyridine, formaldehyde, toluene, water, acetic acid, ammonia.

HIGHLIGHT

- Nanoporous activated carbon was successfully prepared from lapsi seed stone
- In this study, preheating of precursor prior to chemical activation has been reported, and its effect on surface area as well as electrochemical characterization was discussed.
- The chemical activation by phosphoric acid which contribute to have high surface area of >1500 m^2/g, large pore volume.
- As prepared nanoporous AC disclosed excellent vapour sensing ability towards vaporized solvent gases: methanol, acetone, benzene, hexane, pyridine, formaldehyde, toluene, water, acetic acid, ammonia.

* Corresponding author: Armila Rajbhandari (Nyachhyon),
✉ E-mail: armila3@yahoo.com
☏ Tel number: 00977-1-9841243565

G R A P H I C A L A B S T R A C T

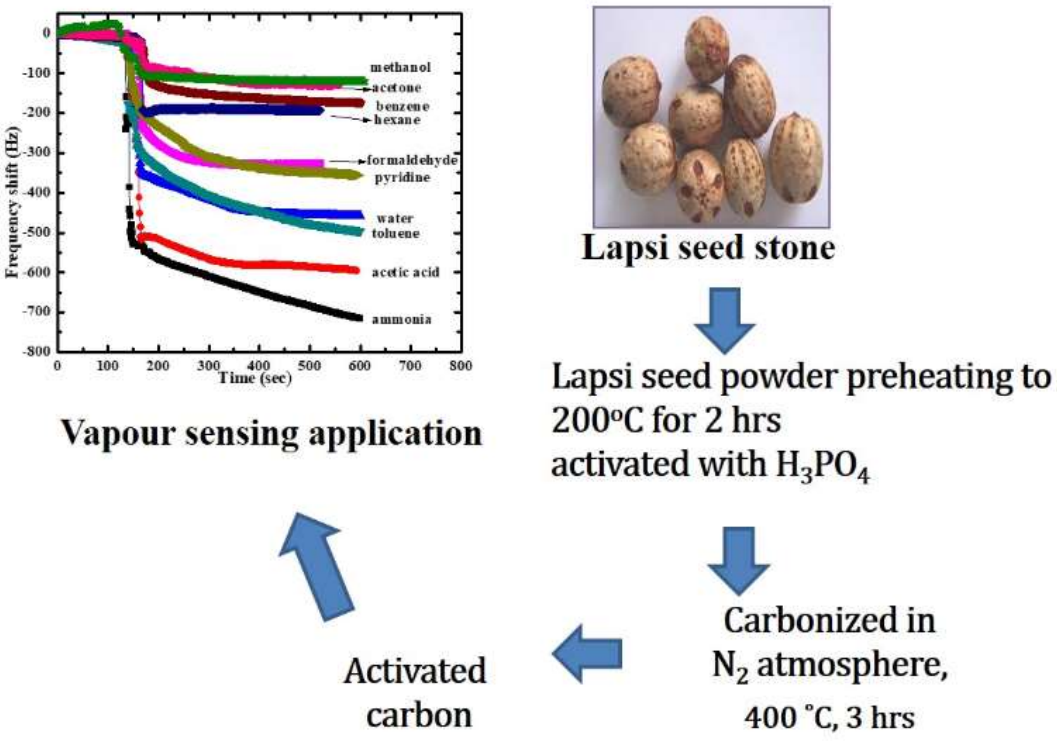

INTRODUCTION

Activated carbon (AC) is reflected as advanced smart functional materials for sensors, capacitors, energy storage and harvesting. The possibility of nano architectonics [1-2] on AC released the novel path way in materials science. The fabrication of sensors, capacitors, efficient solar cells, batteries from nanoporous AC became popular due to their surprising possessions like high specific surface area, large pore volume, good mechanical stability, chemical inertness, and relatively low cost [3]. In the recent years, lignocellulosic carbonaceous materials has been used for the preparation of AC [4]. The literatures reported different eco-friendly low cost lignocellulosic precursors such as almond shell [5], corn cob [6], sugarcane bagasse [7], rice husk [8], waste tea [9], and saw dust [10]. These lignocellulosic materials when carbonized by controlling different parameters like temperature, heating rate, holding time, inert environment, amorphous form of carbon is obtained which is generally porous in nature. However, the porosity can be enhanced by physical as well as chemical activation process which helps to remove tars from interstices of matrix. The activation also supports to create additional porosity on them. In physical activation, carbon precursor is pyrolyzed at high temperature around 1000°C, in absence of oxygen to remove non-carbon species, and followed by exposing to oxidizing atmosphere (CO_2, steam or mixture of both) at temperature around 1000°C to develop porosity by partial etching of carbon. In chemical activation, prior to carbonization, the carbon precursor is impregnated with certain chemicals such as KOH, NaOH, H_3PO_4, $ZnCl_2$, H_2SO_4 [11]. Thus impregnated precursor is then carbonized at slightly lower temperature range of 400-900°C. Here, the chemical agents help for developing porosity in AC via dehydration and degradation of organic precursor. Chemical activation is preferred over physical activation owing to the lower temperature and shorter time needed for materials activation [11]. The yield product is

also high in chemical activation. Moreover, chemical activation generally results in more uniform size distribution. On the basis of pore size, porosity is classified into micropores, mesopores and macropores [12]. Generally, pore size greater than 50 nm are called as macropores whereas pore size less than 2 nm are termed as micropores. On the other hand, the pore size which lies between 2 nm and 50 nm are said to be mesopores. Owing to the presence of micro and mesoporous, the carbons are referred as nanoporous carbon. In this study, we tried to prepare nanoporous activated carbon from locally available lignocellulosic ecomaterials ie, seed of the indigenous lapsi fruit. It is found in hilly region of Nepal. The scientific name of lapsi is *Choerospondias axillaris* which belongs to the family *Anacardiaceae* [13]. These lapsi seeds are considered as agricultural waste and used only as fuel for brick kiln. Hence, in this research work, these lapsi seeds have been used as a precursor for the preparation of AC. Subsequently, these materials were used to investigate their electrochemical performances and the vapor sensing application. In this study, we report preheating of precursor prior to chemical activation and carbonization, and its effect on characteristic surface area as well as electrochemical characterization which is not reported so far.

MATERIALS AND METHODS

Chemicals and instruments

The chemicals like phosphoric acid, used were of (AR) grade and obtained from Merck Company Germany. Distilled water has been used throughout the experiment. Automatic adsorption instrument (Quantachrome, Autosorb iQ) was used to acquire nitrogen adsorption-desorption isotherms in order to get surface area of activated carbon. CHI 850D Workstation (USA) has been used for cyclic voltammetry and chronopotentiometry measurements in order to investigate the electrochemical properties of the carbon samples.

Preparation of Activated Carbon.

Lapsi fruits were collected from hilly region of Kathmandu. The fleshy part was removed and the seed stones **(Fig. 1)** have been obtained after washing several times with distilled water and drying in an electric oven at 110°C. The material was then grinded into fine powder and sieved through 250 µm sized sieve. Thus obtained lapsi seed powder (LSP) sample was divided into 6 parts. First part of the sample which is named as sample (a), second part of the sample is named as sample (b) whereas third part is named as sample (c), fourth part is sample (d), fifth part is sample (e) and sixth part is named as sample (f). These samples were then subjected to carbonization. The details of carbonization condition are given in (**Table 1**).

Fig. 1: Lapsi seed stone

Table1: Carbonization condition

Sample name	Preheating temp (°C)	Preheating Time (hr)	Carbonization temp(°C)	Carbonization time (hr)	H_3PO_4:LSP (wt:wt)
Sa	-	-	400	3	-
S(b-1)	-	-	400	3	(0.9:1)
S(b-2)	-	-	400	3	(1.2:1)
S(b-3)	-	-	400	3	(1.5:1)
S(c-1)	200	1	400	3	(0.9:1)
S(c-2)	200	1	400	3	(1.2:1)
S(c-3)	200	1	400	3	(1.5:1)
S(d-1)	200	2	400	3	(0.9:1)
S(d-2)	200	2	400	3	(1.2:1)
S(d-3)	200	2	400	3	(1.5:1)
S (e)	200	4	400	3	(1.2:1)
S (f)	200	6	400	3	(1.2:1)

Carbonization of Powder Samples

I. Sample (a) was carbonized at 400°C for 3 hrs in an inert nitrogen atmosphere. The carbonized sample was then cooled to room temperature under an inert atmosphere. The cooled sample was then washed 5 times with deionized water. Finally, the sample was dried in an oven at 110°C for 3 hrs and stored in an air tight vessel. This sample was not preheated and chemically activated prior to carbonization (**Table 1**).

II. Sample (b) was again divided into three parts and chemically treated with phosphoric acid in three different ratio of (H_3PO_4: LSP) such as (0.9:1), (1.2:1), (1.5:1) wt:wt and named as S (b-1), S (b-2), S (b-3) respectively. These samples were not preheated prior to carbonization. Thus treated sample was then left for 24 hrs for proper soaking and dried in an oven at 110 °C for 2 hrs. These dried samples were carbonized at 400°C for 3 hrs under inert nitrogen atmosphere. The carbonized sample was then cooled to room temperature under continuous flow of nitrogen. The cooled sample was washed with deionized water for several times. The washings were tested by litmus paper. The washing process was continued till neutral litmus test was observed. Finally, the washed sample was dried in an oven at 110°C for 3 hrs and stored in an air tight vessel for further characterization (**Table 1**).

III. Sample (c) was also divided into three parts and preheated to 200°C for 1 hr prior to chemical activation. Phosphoric acid and LSP was taken in the ratio of (0.9:1), (1.2:1), (1.5:1) wt:wt and named as S (c-1), S (c-2), S (c-3) respectively. These samples were left for 24 hrs for soaking and dried in an oven at 110°C for 2 hrs which were then carbonized in tubular furnace at 400°C for 3 hrs in N_2 atmosphere as described earlier (**Table 1**).

IV. Sample (d) was again divided into three parts and preheated to 200°C for 2 hrs prior to chemical activation. Chemical activation was done by taking phosphoric acid and LSP powder in the ratio of (0.9:1), (1.2:1), (1.5:1) wt:wt. and named as S (d-1), S (d-2) and S (d-3) respectively. The further process of soaking, drying and carbonization has been carried out as described earlier (**Table 1**).

V. Sample (e) and Sample (f) preheated to 200 °C for 4 hrs and 6 hrs respectively prior to chemical activation. Chemical activation was done by taking phosphoric acid and LSP

powder in the ratio of (1.2:1) which were then carbonized in tubular furnace at 400°C for 3 hrs in N_2 atmosphere as described earlier. These samples were named as S(e) and S(f) respectively (**Table 1**).

Nitrogen adsorption - desorption measurements at 77 K were conducted to investigate surface area, pore volume, and pore size distribution of as prepared samples. Electrochemical measurements were performed in a three-electrode cell, in which as prepared activated carbon sample was used as the working electrode, platinum electrode as the counter electrode, Ag/AgCl as reference electrode and H_2SO_4 (1 M) as an electrolyte. The working electrode was fabricated by drop casting method. In this experiment, 5 µL of carbon sample dispersed in water (2 mg/mL) was poured on glassy carbon electrode and dried for 2 hrs at 70°C. Then, 5 µL (0.5 %) nafion binder was added to bind the material. Cyclic voltammetry (CV) and chronopotentiometry measurements were conducted in the potential range of 0 to 0.8 V. The measurements were performed using Electrochemical Analyzer. The specific capacitance (Cs) was calculated from the discharge curve. Mass of AC was calculated by QCM. The frequency of Quartz Crystal Microbalance (QCM) electrode was measured during the adsorption of different solvent vapours.

RESULTS AND DISCUSSION

Surface area determination using Nitrogen Adsorption-Desorption Isotherm

The nitrogen adsorption isotherms for the series of as prepared AC samples are presented in **Fig. 2**. In **Fig. 2**, the adsorption-desorption isotherms of sample S (a), S (b-1), S (d-1), S (d-2) and S (d-3) are given where volume of N_2 gas at STP was plotted as a function of relative pressure (P/P_0).

Figure 2 demonstrates that adsorption-desorption isotherm strongly depends on H_3PO_4 impregnation ratio. Here S (a) did not show any significant nitrogen adsorption in the entire relative pressure range which indicates the absence of porous structure in this sample. However, the significant uptake of nitrogen was observed in sample S (b-1) when the precursor was activated with 0.9:1 (H_3PO_4 : LSP) ratio. The more significant uptake was observed in sample S (d-2). This sample was prepared by preheating 2 hrs prior to activation and then activated with H_3PO_4 with the same ratio i.e., (0.9:1). Here, the curves of sample S (b-1), S (d-2) and S (d-3) showed type IV adsorption behavior according to IUPAC. The initial part of the isotherm was found in low relative pressure region (P/P_0< 0.1) with significant uptake of nitrogen corresponds to adsorption in micro pores. At intermediate and high relative pressures, the isotherms showed some sort of a hysteresis loop.

On the basis of IUPAC, the hysteresis loop is associated with monolayer–multilayer adsorption followed by capillary condensation in narrow slit-like pores. Drastic nitrogen uptake at lower relative pressure region with hysteresis loops at higher relative pressure in the adsorption–desorption curves had given a positive indication of presence of both micro- and mesoporous ie, nanoporous structures in carbon samples.

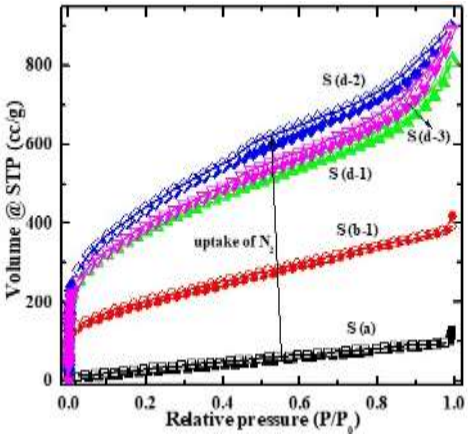

Fig. 2: N_2 adsorption desorption isotherms of sample S (a), S (b-1), S (d-1), S (d-2) and S (d-3)

As can be seen in **Fig. 2**, nitrogen adsorption increases with increasing ratio of impregnation from (0.9:1) to (1.2:1) indicating gradual development of porous structure. Further increase in ratio (1.5:1) caused decreasing adsorption of nitrogen. The decrease in adsorption capacity can be described as deterioration of porous structure which may probably due to destruction of wall between adjacent micropores due to phosphoric acid activation [14]. All phosphoric acid activated carbon samples showed a well-developed porous structure with BET surface area of 1553 m^2/g and total pore volume 2.051 cm^3/g **(Table 2)**. The pore size distribution was calculated by Barrett-Joyner-Halenda (BJH) method and was predicted to be nanoporous. **Table 2** shows the BET surface area and pore volume of S (a), S (b-1), S (b-2), S (d-1), S (d-2) and S (d-3) carbon samples. Sample S (a) has lowest surface area and pore volume which was carbonized only but activation was not done. In comparison to S (a), S (b-1) sample which was activated with H_3PO_4 in the ratio of 0.9:1 showed approximately 5 times greater surface area. The surface area and pore volume was further seemed to be increased (about 2 times) in the sample S (d-1) which was preheated at 200°C for 2 hrs prior to activation and the activation ratio was 0.9:1. Among all six samples, the sample S (d-2) showed highest surface area and pore volume. This sample S (d-2) was that sample which was preheated at 200°C for 2 hrs prior to activation and 1.2:1 was the activation ratio. Sample S (d-3) showed lower surface area than that of S (d-2) which was preheated at 200°C for 2 hrs prior to activation and then activated in the ratio 1.5:1. However, pore volume of this sample was not decreased. Here, it was clearly seen that high impregnation ratio is not favorable for the production of AC having high surface area.

Table 2: Specific surface area and pore volume of AC samples

Sample	Specific Surface area (m^2/g)	Micropore volume (cc/g)	Mesopore volume (cc/g)	Total pore volume (cc/g)
S (a)	126	0.14	0.165	0.305
S (b-1)	680	0.545	0.369	0.914
S (b-2)	831	0.665	0.426	1.091
S (d-1)	1329	1.105	0.749	1.854
S (d-2)	1553	1.256	0.794	2.05
S (d-3)	1386	1.214	0.856	2.07

Table 3: Surface area and pore volume in S(e) and S(f)

Sample	Specific Surface area (m^2/g)	Micropore volume (cc/g)	Mesopore volume (cc/g)	Total pore volume (cc/g)
S (e)	1411	1.192	0.8	1.992
S (f)	1124	0.89	0.561	1.451

From **Table 2**, it was found that preheating time 2 hrs and activation ratio 1.2:1 is favorable condition to have highest surface area as well as pore volume. Then we tried to investigate on effect of preheating time as a function of surface area. The sample S (e) and S (f) was taken in which activation ratio was kept constant, i.e., 1.2:1. Similarly, preheating temperature was also kept constant (200°C) but preheating time was increased from 4 hrs to 6 hrs. The results obtained are tabulated in **Table 3**. It was found that when preheating time was increased to 4 to 6 hrs, the surface area and pore volume get reduced in comparison to S (d-2). It may be due to breakdown of walls in mesoporous forming macropores.

Figure 3 shows a bar diagram of the surface area and pore volume of AC samples S (b-2), S (c-2) and S (d-2), S(e), S(f) to study the effect of preheating time prior to activation and activated in 1.2:1 ratio. From **Fig. 3**, it was observed that the sample without preheating S (b-2) had low surface area of 831 m^2/g and pore volume whereas sample preheated at 200°C for 1 hr prior to activation S (c-2) showed improvement in surface area upto 1141 m^2/g. The surface area and pore volume was further seemed to be increased with increase in preheating time upto 2 hrs, S (d-2). However, it was found to be decreased with further increase in preheating time of 4 hrs and 6 hrs in sample S (e) and S (f) respectively. **Figure 3** further supported that the sample S (d-2) had highest surface area of 1553 m^2/g as well as pore volume of 2.05 cc/g when preheating time was maintained maximum to 2 hrs indicating the porous nature of material. The porosity may be due to escape of P_2O_5 during carbonization and washing steps creating pores. At that time, oxidation of the carbon no more retained. Further increase in preheating time was not favorable for high surface area and pore volume.

Electrochemical Characterization of as prepared Samples

Cyclic voltammetry (CV) and chronopotentiometry techniques were performed to study the electrochemical properties of as prepared nonporous AC samples. Here, as prepared sample was used as an electrode material.

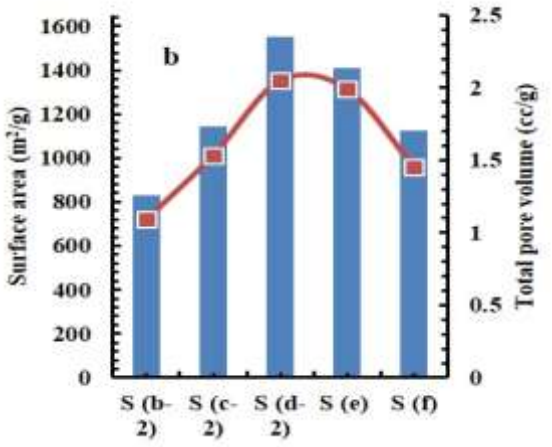

Fig. 3: Distribution of surface area and total pore volume in samples S (b-2), S (c-2) and S (d-2), S(e), S(f).

The experiment was carried out at 0 to 0.8 V potential range against Ag/AgCl reference electrode. One molar sulphuric acid was used as supporting electrolyte.

Cyclic Voltammetry (CV)

Figure 4 shows cyclic voltammograms of S (a), S (b-1), S (d-1) and S (d-2) conducted at different scan rates (5, 10, 20, 50, 80 and 100 mV/s) using potential window of (0 to 0.8 V) in 1 M H_2SO_4 electrolyte. As can be seen in **Fig. 4**, there is a rapid current response to the applied voltage in all cases. In S (a) (**Fig. 4 (a)**), the current response was found to be quite low resulting charging current of only about 3 A/g at scan rate 100 mV/s whereas in sample S (b-1) (**Fig. 4 (b)**), the current response was found to be increased. It may be due to high surface area as well as pore size availability for charge accumulation in the formation of electrical double layer. The further increased in current response can be seen in sample S (d-1) (**Fig. 4 (c)**) in comparison to S (b-1) (**Fig. 4 (b)**). In this case also sample S (d-1) has higher surface area than sample S (b-1). Next sample S (d-2) (**Fig. 4 (d)**) showed slight increase in current response than in S (d-1) (**Fig. 4 (c)**) as there is not much difference in surface area in these two samples. However, sample S (d-2) has displayed higher surface area and pore volume as well as meso and microporous structure. Due to such properties, it was easier for diffusion of electrolyte ion and hence showed higher current response or current density of 9 A/g in 5 mV/s scan rate in CV curve. All these electrochemical properties indicated the capacitive behavior of the material.

On the basis of curves shown in **Fig. 4**, it can be evidenced that the current response by the material increases with increase in scan rate from 5 to 100 mV/s. As a result of this, the specific capacitance was found to be decreased at higher scan rate. The pore structure where solvated ions interact between pore walls is responsible for the major contribution to capacitance value. The decrease in capacitance at higher scan rate is related to the fact that the electrolyte gets shorter diffusion time inside the pores [10].The shape of curves were found to be almost rectangular which is the indication of electrical double layer capacitor [15]. It is nearly ideal EDLC behavior. Here, the electrolyte ion diffusion may be prevented by the migration force as well as polarized resistance. This was the reason which made CV curve slightly different from ideal rectangular shape. Besides this, it is mirror symmetrical even at high scan rate. This type of nature is the evidence of the reversibility of the sample. The rectangular CV curve without pseudocapacitance reveals that the samples show capacitive behavior in which energy storage phenomenon is purely electrostatic.

Chronopotentiometry

Charge-discharge measurements were carried out by chronopotentiometry. The experiment was tested in the potential range of 0 to 0.8 V against Ag/AgCl reference electrode at different current densities. On the basis of total mass on electrode, the charge-discharge current density, was varied from 1 to 10 A/g. **Figure 5** shows the charge - discharge curve (5 cycles) of sample S (d-2) at current density 1 A/g whereas **Fig. 6** shows charge-discharge curve of sample S (a), S (b-1), S (d-1) and S (d-2) at current density 1 A/g.

Figure 5 showed the good stability performance of the S (d-2) electrode and curves are almost symmetrical indicating the reversibility of the electrode as well as double layer capacitive behavior. The sample S (d-2) (**Fig. 6**) displayed the longer discharge time (162.11 s) whereas sample S (a) shows shorter discharge time (23.79 s) at current density 1 A/g.

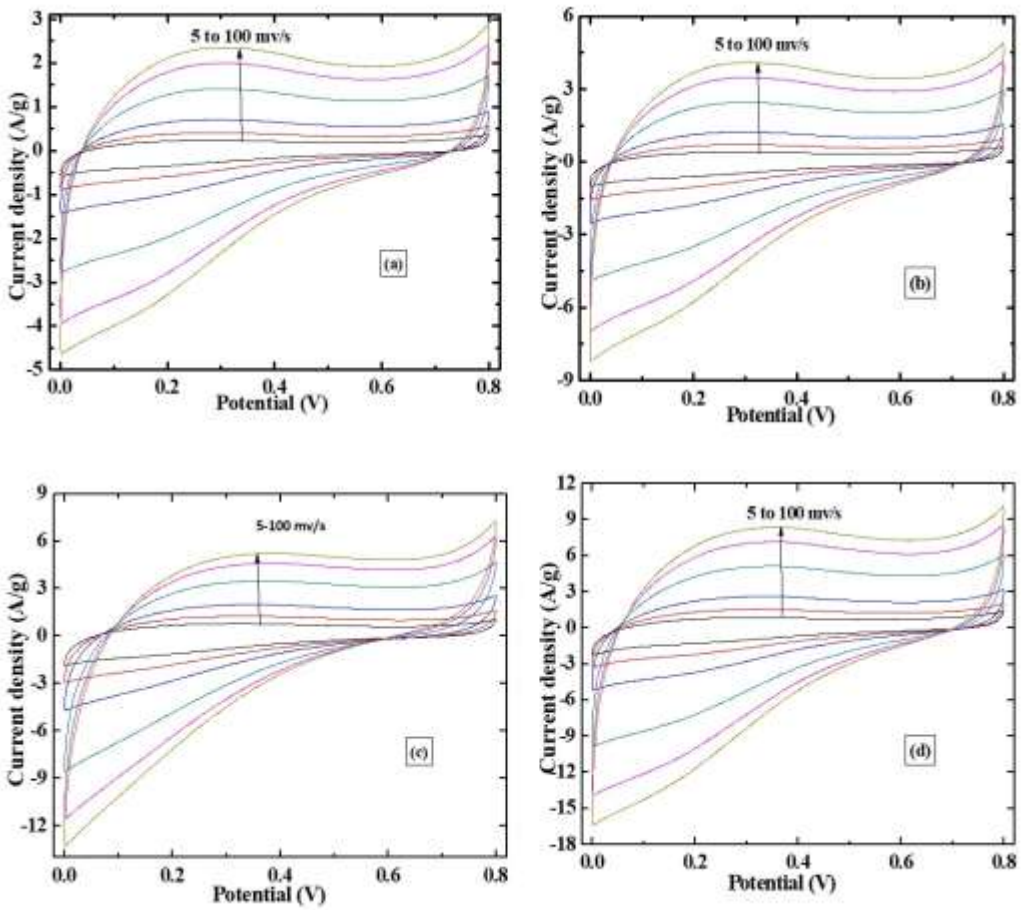

Fig. 4: Cyclic voltammogram of activated carbon samples **(a):** S (a), **(b):** S (b-1), **(c):** S (d-1) and **(d):** S (d-2) at 5, 10, 20, 50, 80 and 100 mV/s scan rates.

The shorter time of discharge may be due to low surface area as the sample was prepared without chemical activation. Such a low surface area makes less availability of electrolyte ion for charge accumulation resulting shorter time for charge discharge. On the other hand, sample S (d-2) possess high surface area with nanoporous structure. This property makes easy accessibility for charge accumulation at large area of electrode leading to longer time of discharge. The surface area of S (d-2) is twice as high as S (b-1) (**Table 2**). In the same way, the discharge time between these samples were also found to be twice (**Fig. 6**). Similarly, **Fig. 7** showed typical linear discharge curves of sample S (a), S (b-1), S (d-1) and S (d-2) at different current densities such as 1, 2, 3, 4, 5 and 10 A/g. These linear curves indicate well balanced charge storage in all the prepared samples [16].

Then the specific capacitance values of samples S (a), S (b-1), S (d-1) and S (d-2) were calculated using equation (1) and the values were tabulated in **Table 4**.

$$Cs = I \times t/V \times m \qquad \textbf{(1)}$$

Here, I is charging and discharging current in ampere. t is discharging time in second. V is the potential across the capacitor in volts. m is mass of active material in gram. Cs is specific capacitance in farad per gram.

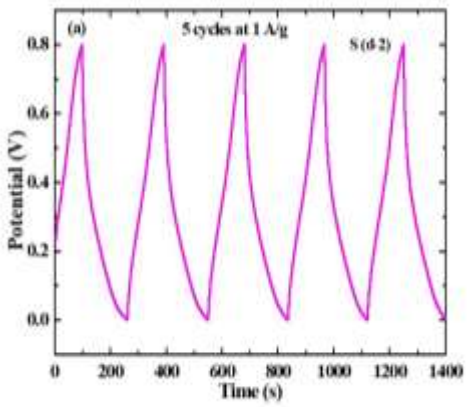

Fig. 5: Charge-discharge cycles of sample S (d-2) at current density 1A/g.

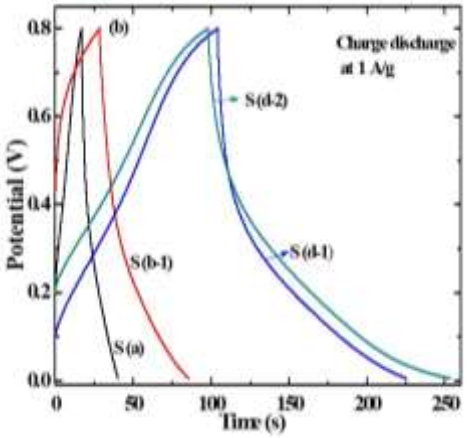

Fig. 6: Charge-discharge curve of sample S (a), S (b-1), S (d-2) and S (d-3) at current density 1A/g.

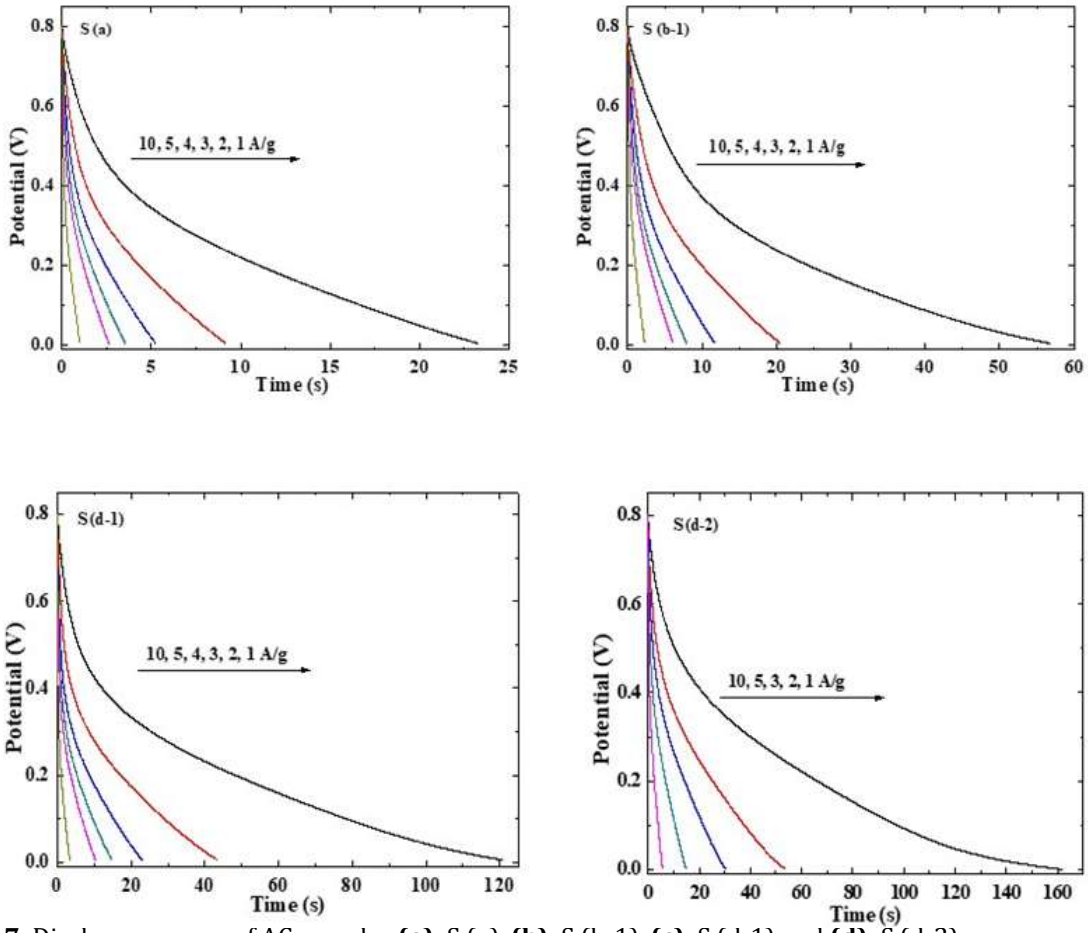

Fig. 7: Discharge curves of AC samples **(a)**: S (a), **(b)**: S (b-1), **(c)**: S (d-1) and **(d)**: S (d-2) at different current densities.

Table 4: Specific capacitance value at different current densities.

Sample	Specific capacitance at different current densities (F/g)					
	1 A/g	2 A/g	3 A/g	4 A/g	5 A/g	10 A/g
S (a)	29.73	23.32	19.98	18	16.63	12.75
S (b-1)	73.01	52.40	44.85	40.45	39.06	29.12
S (d-1)	155.87	111.23	88.31	75.25	66	43.12
S (d-2)	202.63	134	113.77	-	93.1	70.62

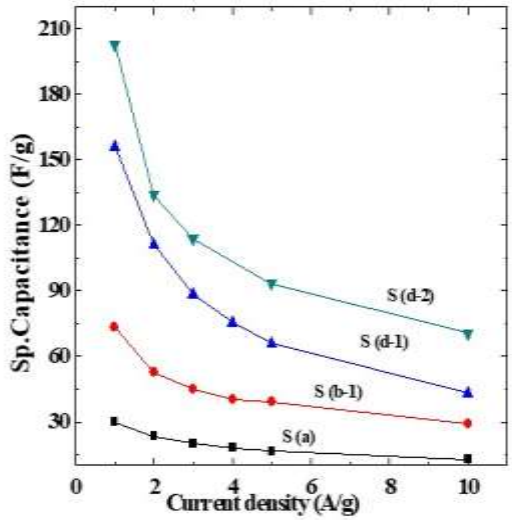

Fig. 8 : Specific capacitance of sample S (a), S (b-1), S (d-2) and S (d-3) as a function of current density

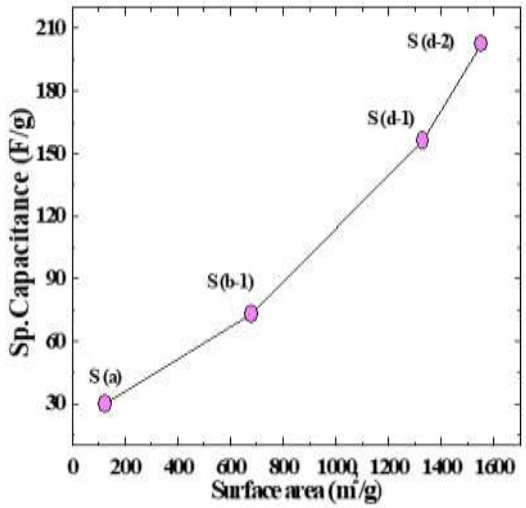

Fig. 9: Specific capacitance of sample S (a), S (b-1), S (d-2) and S (d-3) as a function of surface area.

The plots of specific capacitance (F/g) as a function of current density (A/g) and specific capacitance (F/g) versus surface area (m^2/g) are shown in **Fig. 8 and 9. Figure 8** and **9** shows that shrinkages of specific capacitance with increase in current density. At low current density, the diffusion of ion from the electrolyte to sample get sufficient time to access into the large surface area of electrode, as a consequence, a higher specific capacitance was attained. With the increase of current density, the effective interaction between the ions and electrode got reduced resulting in lower value of capacitance. As can be seen in **Fig. 8**, sample S (a) showed less specific capacitance value (29.73 F/g) at current density 1 A/g and this value decrease with increase in current density. In S (d-2) showed maximum specific capacitance value (202.63

F/g) at current density 1 A/g. However, it was gradually decreased to 70.62 F/g at current density 10 A/g but was equal with the sample S (b-1) at current density 1 A/g. It showed that at low current density, specific capacitance is quite high. Similar trend can be observed in sample S (d-1). In sample S (b-1), specific capacitance is higher (73 F/g) at current density 1 A/g than that of sample S (a) (29.73 F/g) which was not activated. However, specific capacitance value of S (b-1) was found to high at current density 10 A/g than other samples. Again, the specific capacitance was plotted as a function of surface area (m^2/g) (**Fig. 9**) showing the higher specific capacitance sample having large surface area. It exhibited high surface area with large volume of micro and mesopores favors the better electrolyte contact and supports the accumulation of more electrolyte ions in the pores and hence increases the charge storage density. Though the surface area is a main factor for the enhanced electrochemical performance of the material, the other parameters like electrical conductivity, presence of surface functional groups also have some effect on specific capacitance. Here, it was found that AC sample S (d-2) in which LSP was preheated at 200°C prior to activation for 2 hrs and activated by H_3PO_4 in the ratio 1.2:1 showed high surface area of 1553 m^2/g. This sample also displayed the highest capacitance value of 202 F/g at current density 1 A/g.

Cyclic performance

To investigate the life cycle or stability of material, the cyclic performance of sample S (d-2) was carried out upto 1000 cycles at current density of 5 A/g which is demonstrated in **Fig. 10**. In **Fig. 10**, the initial specific capacitance value was found to be 93 F/g whereas capacitance value after thousandth cycle was found to be 86 F/g. It indicated that the electrode material exhibited stable performance upto 1000 cycles with a loss of 7.5%.

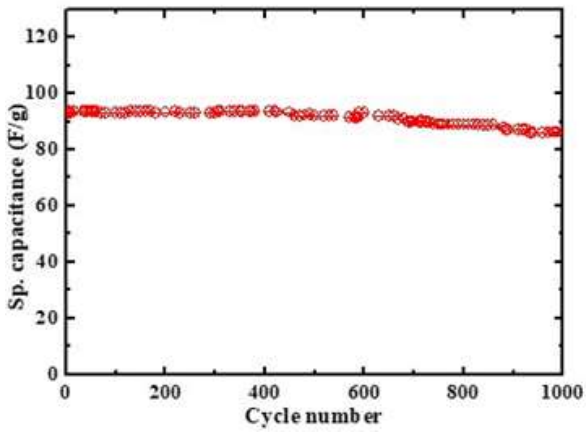

Fig. 10: Cyclic performance test for sample S (d-2) at current density 5 A/g.

This is positive response and also revealed that the electrode material S(d-2) meet the requirements of high stability and good rate capability.

Vapor Sensing Application of AC in Different Solvent Media

Nano-porous materials having high surface area and pore volume are potential substance that can be used to sense organic, aqueous and non-aqueous solvents by vapor sensing technique. Here, quartz crystal microbalance (QCM) method was used to investigate vapor sensing ability of carbon sample in different solvent vapors. For this investigation, QCM sensor was designed by deposition of sample on QCM electrode. The organic solvents that have been used to investigate vapor sensing efficiency are as follows: short chain aliphatic alcohol (methanol), toxic aromatic solvents (benzene, toluene and pyridine, acid (acetic acid), aldehyde (formaldehyde), ketone (acetone), hexane, aqueous solvent (water) and non-aqueous solvent (ammonia). Here, sample S (d-2), which was prepared by preheating LSP at 200°C for 2 hrs prior to chemical activation and then activated in the ratio of 1.2:1 (H_3PO_4:LSP), was used to investigate the vapor sensing as well as good electrochemical properties.

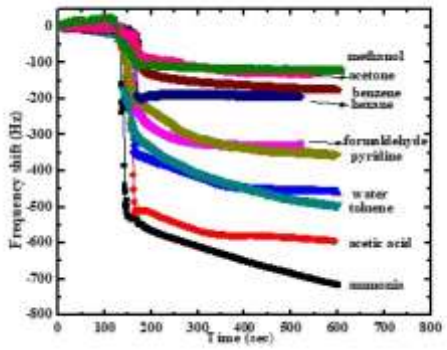

Fig. 11: A plot of frequency shift in Hz as a function of time in second when the sample S(d-2) was exposed to vaporized solvent gases: methanol, acetone, benzene, hexane, pyridine, formaldehyde, toluene, water, acetic acid, ammonia.

In **Fig. 11** the vapor sensing efficiency of carbon sample S (d-2) in different solvents were shown by plotting frequency shift in hertz as a function of time in second. Here, a QCM sensor was exposed to different solvent vapors. As can be seen in **Fig. 11**, the frequency shift (Δf) occurred immediately <150 s when the sample was exposed to vaporized solvent gas. This showed that the sample responses rapidly to the solvent vapors. Though, the response depends on the nature of solvent molecules.

Here, to check the sensing ability for solvent (methanol), first the frequency (f) of QCM sensor was recorded upto 2 minutes and then after 2 minutes sensor was exposed to methanol solvent vapor in closed system. The frequency was recorded again. The significant change in frequency (Δf) approximately about 100 Hz was observed. After this decrease in frequency, it was found that the frequency remained constant which was obvious in **Fig. 11**.

The constant frequency was due to attainment of equilibrium. After this measurement, the electrode was exposed to air to desorb the solvent vapor. After desorption, the frequency of QCM sensor was recorded again in order to attain the initial frequency value.

Then, other solvents were also taken and similar procedure has been applied as in methanol solvent. In acetone, the change in frequency (Δf) was found to be ~125 Hz. In the same way, (Δf ~ 175 Hz) was recorded for benzene. The frequency shift (Δf) of ~ 193 Hz, 328 Hz, 355 Hz, 458 Hz, 496 Hz, 609 Hz and 700 Hz was observed for solvent hexane, formaldehyde, pyridine, water, toluene, acetic acid and ammonia respectively at room temperature. The frequency shift (Δf) values of all solvents are tabulated in **Table 5**.

Table 5: Frequency shift (Δf) values for different solvents

Solvent	Frequency Shift (Δf) in Hz
Ammonia	700
Acetic acid	609
Toluene	496
Water	458
Pyridine	355
Formaldehyde	328
Hexane	193
Benzene	175
Acetone	125
Methanol	100

From **Table 5**, it has been obtained that the QCM electrode prepared from S(d-2) showed excellent sensing affinity towards ammonia vapor as indicated by higher Δf value of approximately 700 Hz than other solvents. However, sensor showed longer time to attain equilibrium. In comparison to ammonia, acetic acid showed fast attainment of equilibrium with frequency shift (~

609 Hz). So, the repeatability test was also carried out with acetic acid. The result showed that the electrode has low affinity towards methanol vapor as the frequency shift value was lower of about100 Hz. This lower frequency shift (Δf) for methanol indicates that the sensor is not suitable for sensing aliphatic alcohol. However, this frequency shifts (~100 Hz) was found to be better in comparison with the literature value ~16 [17]. However, the sensing ability was found to be slightly greater in acetone, benzene and hexane. The sensing ability was found to be better in pyridine and formaldehyde. When frequency shifts of benzene 175 Hz and pyridine 355 Hz were compared with the literature values of benzene ~ 28 and pyridine ~90 [17], it is appreciated to be significantly high. Similarly, toluene, one of the very toxic aromatic solvent in which, (Δf) ~ 496 Hz, that demonstrates suitability of material for sensitivity. The frequency shifts of ~458 and 609 Hz in water and acetic acid showed far better adsorption than methanol, acetone, benzene, hexane and pyridine. On the basis of QCM test, it may be concluded that the nanoporous activated carbon having high surface area and high pore volume, has a high capability to sense the vapour.

Repeatability Test

Though, the QCM sensor was allowed for adsorption and desorption of solvent vapors simultaneously, for further confirmation whether the adsorbed gas will desorb or not and how many cycle does the sensor work properly, the repeatability test was carried out. The result for repeatability test is demonstrated in **Fig. 12**.

In **Fig. 12**, downward filled arrow (↓) indicates the adsorption process while upward dash arrow (↑) indicates the desorption process. In the similar way, horizontal filled arrow (→) indicates the time required to attain stable frequency while adsorbing the vapor whereas horizontal dash arrow (→) indicates the time required to attain stable frequency before adsorption of vapor molecules. From **Fig. 12**, it was found that all the adsorbed vapors were easily desorbed when the QCM sensor was exposed to air. This repeatability test is useful to examine the sensor that can be applied for many cycles during sensing the solvent vapor.

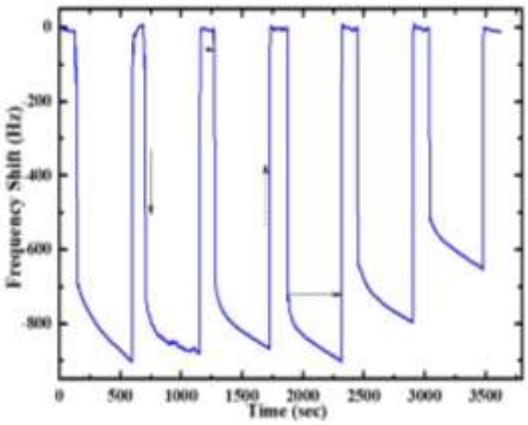

Fig. 12: Repeatability test for acetic acid solvent vapor into carbon sample S (d-2).

CONCLUSION

Nanoporous activated carbon was successfully prepared from lapsi seed stone by phosphoric acid activation and was carbonized at 400°C in tubular furnace in an inert atmosphere of nitrogen. The activation ratio of (H_3PO_4:LSP) was varied from (0.9:1) to (1.5:1). The optimum activation ratio was found to be (1.2:1). Nitrogen adsorption-desorption isotherm study showed that activation ratio and preheating time has significant influence. Sample which was preheated at 200°C for 2 hrs prior to activation and the activation ratio (1.2:1) showed highest surface area of 1553 m^2/g and pore volume 2.05 cc/g. Rectangular shaped cyclic voltammogram showed the electrical double layer capacitive (EDLC) behavior. The samples also showed fast electrolyte ion diffusion with high current response of the sample S (d-2). The increase in capacitance value could be attained by decreasing the scan rate of CV and lowering current density as well. From cyclic performance test, it was concluded that as prepared sample S

(d-2) is stable upto 1000 cycles. The as prepared AC sample derived from lapsi was successfully applied in vapor sensing of different organic solvents. The sample showed rapid response to the solvent vapors. The selectivity of sensing was found to be increasing in the order: methanol < acetone < benzene < hexane < pyridine < formaldehyde < toluene < water < acetic acid < ammonia. QCM electrode prepared from (S(d-2)) showed excellent sensing affinity towards ammonia vapor as indicated by higher Δf value of approximately 700 Hz. From this study, it was concluded that AC sample could be effectively used in sensing vapors of organic solvents.

ACKNOWLEDGEMENT

We gratefully acknowledge National Institute of Materials Science (NIMS), Japan for providing laboratory facilities for characterization of carbon samples. Sandhya Acharya would like to express sincere thanks to NIMS-Japan for providing NIMS Internship.

REFERENCES

[1] M. Ramathanan, L.K. Shrestha, T. Mori, Q. Ji, J.P. Hill and K. Ariga, Amphiphile Nanoarchitechtonis from basic physical chemistry to advanced applications. Physical Chemistry Chemical Physics, 15 (2013) 10580-10611.

[2] K. Ariga, A. Vinu, Y. Yamauchi, T. Mori, Q. Ji and J.P. Hill, Nanoarchitectonics for mesoporous materials, Bulletin of. Chemical Society, Japan, 85 (2012) 1.

[3] L. L. Zhang and X. S. Zhao, Carbon based materials as supercapacitor electrodes, Chemical Society Reviews, 38 (2009) 2520–2531.

[4] M. Sharon and Sharon M., Nano forms of carbon and application, Monad nanotech Pvt. Ltd , India, 2007.

[5] M. Plaza, C. Pevida, C. Martin, J. Fermoso, J. Pis and F. Rubiera, Developing almond shell-derived activated carbons as CO_2 adsorbents, Separation Purification Technology, 71 (2010) 102–106.

[6] Q. Cao, K. C. Xie, Y. K. Lv and W. R. Bao, Process effects on activated carbon with large specific surface area from corn cob. Bioresearch Technology, 97 (2006) 110–115.

[7] B. S. Girgis, L. B. Khalil and T. A. M. Tawfik, Activated carbon from sugar cane bagasse by carbonization in the presence of inorganic acids Journal of Chemical Technology. And Biotechnology, 61 (1994), 87-92.

[8] Y. Nasehir, M. F. Pakir, M. Latiffa, I Abustana and M. A. Ahmadb, Effect of preparation conditions of activated carbon prepared from rice husk by $ZnCl_2$ activation for removal of Cu (II) from aqueous solution International Journal of Engineering Technology, 10 (2010) 27–31.

[9] B. Amarasinghe and R. Williams, Tea waste as a low cost adsorbent for the removal of Cu and Pb from wastewater Chemical Engineering Journal, 132 (2007) 299–309.

[10] D. Shrestha, S. Maensiri, U. Wongpratat, S.W. Lee, A. Rajbhandari (Nyachhyon), Shorea robusta derived activated carbon decorated with manganese dioxide hybrid composite for improved capacitive behaviors, Journal of Environmental Chemical Engineering, 7 (2019) 103227.

[11] A. R. Mohammad, M. Mohammadi and G.N. Darzi, Preparation of carbon molecular sieve from lignocellulosic biomass: A review, Renewable and Sustainable Energy Reviews, 14 (2010) 1591-1599.

[12] H. March and R. F. Reinoso, Activated Carbon, Elsevier, Amsterdam, 2006.

[13] Poudel K. C., Domesticating Lapsi, Choerospondias axillaris Roxb. (B. L. Brutt & A. W. Hill) for fruit production in the middle mountain agroforestry systems in

Nepal. Himalayan Journal of Science, 1 (2003) 55–58.

[14] N. V. Sych, S. I. Trofymenko, O. I. Poddubnaya, M.M. Tsyba, V. I. Sapsay, D.O. Klymchuk , and A.M. Puziy, Applied Surface Science, 261 (2012) 75–82.

[15] W. Chaikittisilp, M. Hu, H. Wang, H. S. Huang, T. Fuita, K. C. W. Wu, L. C. Chen, Y. Yamauchi and K. Ariga, Chemistry Communication, 48 (2012) 7259–7261.

[16] R. R. Salunkhe, Y. Kamachi, N. L. Torad, S. W. Hwang, Z. Sun, S. X. Dou, J. H. Kim and Y. Yamauchi, Journal of Material Chemistry A, 2 (2014) 19848–19854.

[17] R. Rajbhandari, L. K. Shrestha, B. P. Pokharel and R. R. Pradhananga, Development of nanoprous structure in carbons by chemical activation with zinc chloride, Journal of Nanoscience and Nanotechnology, 13 (2013) 2613– 2623

HOW TO CITE THIS ARTICLE

Armila Rajbhandari (Nyachhyon) and Sandhya Acharya, Preparation, Electrochemical Characterization and Vapour Sensing Application of Nanoporous Activated Carbon derived from Lapsi, Prog. Chem. Biochem. Res. 2020, 3(4) (2020) 350-365.

DOI: 10.22034/pcbr.2020.113921

URL: http://www.pcbiochemres.com/article_113921.html